

A PNIPAM-based fluorescent nanothermometer with ratiometric readout†

Chun-Yen Chen and Chao-Tsen Chen*

Received 16th October 2010, Accepted 8th November 2010

DOI: 10.1039/c0cc04450d

A novel molecular thermometer with ratiometric fluorescence readout was designed and synthesized. Within a sensing temperature range of 33 to 41 °C, the fluorescence color of the nanothermometer changes from blue to green. The ratiometric change magnitude is about 8.7-fold, rendering the visual differentiation of color by the naked eyes feasible.

Among manifold stimuli-responsive polymeric materials, molecular thermometers have received increasing attention in recent years for many reasons.¹ For instance, they hold great promise in identifying infected or cancerous cells, which have lower or higher physiological temperatures than normal ones.^{2a} Engineering applications urgently require novel thermosensitive devices for minute regions and harsh milieu, in which conventional thermometers are inapplicable.^{2b}

Poly *N*-isopropylacrylamide (PNIPAM) materials^{2–5} have been considered as promising candidates for molecular thermometers in several years. Around a specified temperature, commonly referred to as a lower critical solution temperature (LCST), PNIPAMs in aqueous solutions undergo a coil-to-globule phase transition due to the destruction of intermolecular hydrogen bonding between polymer chains and water.^{1a} To visualize the temperature-induced morphological transition, many chromophores³ and fluorophores^{2,4,5} have already been incorporated in PNIPAM-based molecular thermometers. Among them, fluorescence sensing is highly valued since it can provide a more sensitive, selective and real-time detection than other analysis methods. For instance, Uchiyama *et al.*² developed a series of fluorescent molecular thermometers based on PNIPAM materials covalently labeled with the polarity-sensitive oxadiazole fluorophores. At lower temperatures, the oxadiazole fluorophores remain in well-swollen and hydrophilic milieu, resulting in a weak fluorescence, whereas at higher temperatures, the shrinkage of PNIPAMs is accompanied with an increase in fluorescence intensity. However, this kind of fluorescent sensing mechanism still incurs certain problems including excitation source fluctuations, photobleaching, and a discrepancy in dye content among batches.⁶ Moreover, for a single-emission readout, distinguishing between the slight changes in intensities either by visual inspection or with the aid of an instrument is rather difficult. In contrast with single-emission fluorescent probes, a ratiometric fluorescent one can display a self-calibrating readout and overcome difficulties encountered by the conventional

fluorescent probes, ultimately providing more robust signals.⁵ It is indeed an emerging trend in developing dual-emission and wavelength-ratiometric sensing schemes.^{6,7}

This communication demonstrates a sensitive, reversible, and self-calibrating ratiometric fluorescent nanothermometer functioning in the aqueous media. To conform with the ratiometric sensing capabilities, a fluorophore with different emission colors in swollen and shrunken state should be embodied in the polymeric materials. 3-Hydroxyflavones (3-HFs), which display dual-band emissions associated with normal excited state intramolecular charge transfer (denoted as either ESICT or N*) and tautomer excited state intramolecular proton transfer (denoted as either ESIPT or T*), adhere to the requirements exactly.^{6,8} In polar and aprotic solvents, 3HFs display a greenish fluorescence emission originating from the coupled ESICT/ESIPT processes. Whereas the ESIPT reaction is suppressed in highly polar, protic solvents, resulting in a dominative blue fluorescence emission. With this as preamble, 3-hydroxyflavone labeled PNIPAM nanogel (3HF-nanogel), which can signal temperature changes in aqueous media with dual fluorescent emissions, is envisioned. Its sensing mechanism as well as the ratiometric feature are schematically depicted in Fig. 1a.

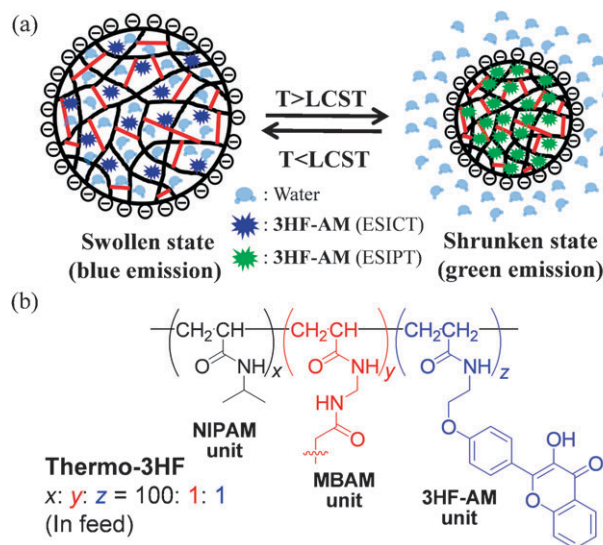


Fig. 1 (a) The swollen state of 3HF-nanogel emits blue fluorescence in aqueous media. Whereas the local temperature exceeds the LCST of nanogels, the nanogels shrink accompanied with green emission. (b) The chemical compositions of nanogels: thermoresponsive NIPAM unit, crosslinker MBAM unit, and 3HF-AM fluorescent unit in various ratios. In the case of Thermo-3HF, an optimized molar ratio of NIPAM, MBAM, and 3HF-AM is 100 : 1 : 1.

Department of Chemistry, National Taiwan University, No. 1, Sec. 4, Roosevelt Road, Taipei, 10617 Taiwan, R.O.C.
E-mail: chenct@ntu.edu.tw

† Electronic supplementary information (ESI) available: Experimental details. See DOI: 10.1039/c0cc04450d

The monomer containing 3-hydroxyflavone fluorophore, denoted as **3HF-AM**, was synthesized (see ESI Scheme S1 and the synthetic procedures†) and its fluorescence behavior in response to different ratios of water and dimethylsulfoxide (DMSO) was characterized. To our expectation, the fluorescence colors gradually change from blue to green in the increasing DMSO content (see ESI Fig. S1†). **3HF**-nanogel was therefore prepared by slightly modifying the emulsion polymerization method delineated by Uchiyama *et al.*^{2a} However, the poor water-soluble fluorescent 2-[4-(3-hydroxy-4-oxo-4H-chromen-2-yl)phenoxy]ethylacrylamide (**3HF-AM**) prevented its effective incorporation into polymer chains during polymerization in an aqueous medium, leading to fluorescently silent thermo-responsive polymers. Following the screening of a series of solvent compositions and the initiators, the optimized reaction condition was determined (see ESI Table S1 for further details†). By using aqueous DMF solution (DMF/H₂O = 7/13) as the reaction solvent, random copolymerization of NIPAM, *N,N'*-methylenebisacrylamide (**MBAM**), and **3HF-AM** in a molar ratio of 100 : 1 : 1 was conducted at 70 °C for 4 h in the APS/TMEDA redox initiator system to afford **Thermo-3HF** (see Fig. 1b). It is noteworthy that 1 mol% crosslinker **MBAM** and high equivalent anionic initiator **APS** were used to fabricate nano-sized particles and enhance the water solubility of the resulting nanogels preventing precipitation.^{2a} The structure and the chemical composition of the synthesized copolymer **Thermo-3HF** were summarized in ESI Fig. S2 and Table S1, respectively.†

To confirm the nano-sized nature and temperature-induced morphological transitions of **Thermo-3HF**, dynamic light scattering (DLS) and transmission electron microscopy (TEM) were conducted and analyzed at various temperatures (Fig. 2a). DLS measurement indicates a two-stage shrinkage upon heating of **Thermo-3HF**. First, a substantial shrinkage occurs from 32 to 36 °C. The phenomenon appears to be attributed to the contraction of the main skeleton in polymers. Thereafter, a slight shrinkage occurs from 36 to 40 °C, which is viewed as a result of the contraction and rearrangement of the fine structures in polymers. The transition range (*i.e.* 32–40 °C) is generally consistent with that derived from the turbidimetric methods (see ESI Fig. S3 for further details†). A TEM image shown in Fig. 2b indicates that **Thermo-3HF** exists in uniform

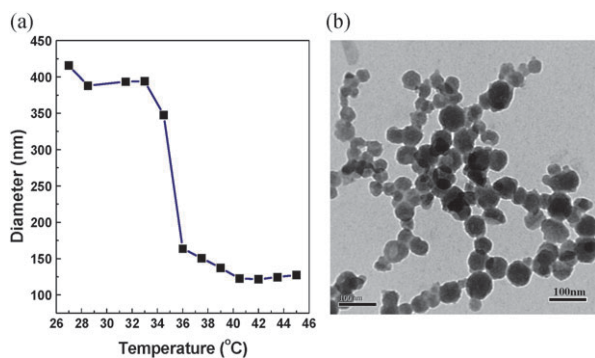


Fig. 2 (a) A correlation between the temperatures and particle sizes of **Thermo-3HF** in an aqueous solution (0.002 w/v%), as examined by dynamic light scattering measurements. (b) A TEM image of **Thermo-3HF**.

round particles and the averaged diameter in the dried state is *ca.* 50–70 nm, which is much smaller than that (*ca.* 400 nm at ambient temperature) obtained from hydrodynamic DLS measurements.

For the proof-of-concept of the nanothermometers with a ratiometric fluorescent readout, the fluorescence behavior of **Thermo-3HF** in different pHs including physiological conditions (pH = 7.4 PBS buffer) at various temperatures was investigated. The results indicate that the fluorescence profiles are similar from acidic to slightly basic conditions. Fig. 3a illustrates the relationship between the fluorescence responses of **Thermo-3HF** in deionized water and the temperatures of the milieu (similar results under physiological conditions were included in ESI Fig. S4†). **Thermo-3HF** displays two-band fluorescence distribution changes when heating from 22 to 52 °C, in which a decline of the ESICT-band was accompanied with the ascent of the ESIPT-band in response to the temperature rise. Moreover, the wavelengths of two-band maximum emission shift from 436 to 423 nm in the ESICT band, and from 508 to 538 nm in the ESIPT band. It is noted that larger **3-HFs'** two-band separation in a more hydrophobic microenvironment coincides with previous work that attempted to verify the existence of H-bond **3HFs** in a hydrophilic solvent.⁹ The observation provides adequate evidence that the ratiometric transition in fluorescence indeed originates from the hydrophilic–hydrophobic conversion in the micro-environment.

Fig. 3b displays the normalized ratios of integrated intensities of the ESIPT and ESICT bands (see ESI for detailed data processing†). Notably, the fluorescence emission of **Thermo-3HF** displays a drastic ratiometric transition, a 8.7-fold leap (Fig. 3b), when the local temperature rises from 33 to 41 °C. The transition temperature observed by fluorescence is in accordance with what is obtained from DLS. Moreover, **Thermo-3HF** displaying an excellent linear relationship between 33 °C and 41 °C warrants its applications in intracellular imaging. The insets of Fig. 3b show the fluorescence photoimages of **Thermo-3HF** dispersed in water at *ca.* 25, 32, 34, 36, 38, and 50 °C. Below the LCST

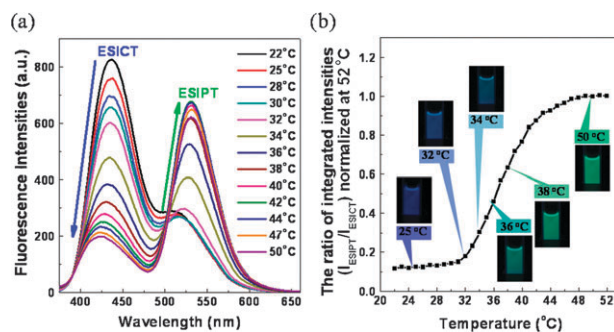


Fig. 3 (a) Overlaid fluorescence spectra of **Thermo-3HF** in an aqueous solution (0.01 w/v%) at various temperatures; excitation wavelength: 355 nm. Every spectrum was acquired after reaching equilibrium. (b) A correlation between the temperatures and normalized ratios of integrated intensities of ESIPT and ESICT bands of **Thermo-3HF**. The data used in (b) is derived from the spectra of (a). The insets show the corresponding fluorescence images at 25, 32, 34, 36, 38 and 50 °C, respectively.

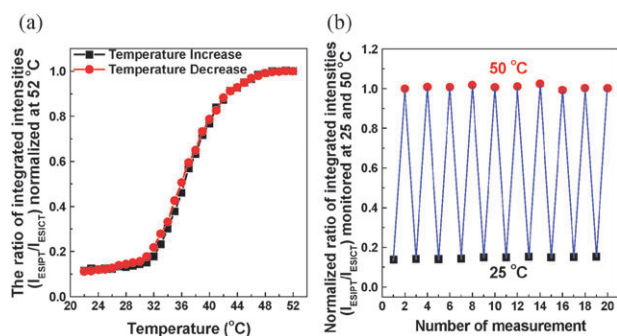


Fig. 4 (a) Single-run and (b) multiple-run reversibility experiments of the fluorescence responses of **Thermo-3HF** to temperature variation. All experimental conditions and data processing are the same as those shown in Fig. 3.

of **Thermo-3HF**, it swells well in the aqueous medium, subsequently providing a highly polar and protic local environment around **3HF** and leading to an ESICT-dominant blue fluorescence emission. Around the LCST, **Thermo-3HF** undergoes a significant phase transition with an increase in temperature, resulting in a more hydrophobic shrunken state, as reflected in the intensity redistribution of two emission bands. The ESICT-related blue fluorescence emission band gradually decreases in intensity with an increasing temperature, whereas the ESIP-related green fluorescence emission band gradually increases in intensity with an increasing temperature. Eventually, **Thermo-3HF** exhibits an ESIP-dominant green fluorescence emission when above the LCST. The color changes in the sensitive range are rather apparent rendering the differentiation of the emission colors by visual detection feasible. Additionally, the ratios of integrated intensities of the ESIP and ESICT bands can be envisioned as a sensitive indicator of microenvironmental temperature.

The reversibility of **Thermo-3HF** was also examined. Fig. 4 shows the single-run and multiple-run reversibility experiments of the fluorescence responses of **Thermo-3HF** to temperature variation. The results indicate that no hysteresis exists during a cycle of heating and cooling (Fig. 4a) and no declining signal occurs during multiple-run tests, monitoring the ratios of integrated fluorescence intensities at 25 and 50 °C (Fig. 4b). The excellent reversibility can be attributed to a highly hydrophilic, ionic surface of **Thermo-3HF**, which prevents individual nanogels from incurring severe intermolecular aggregation through electrostatic repulsion.^{2a} High temperature resolution as well as high availability are thus achieved.

In summary, this work demonstrates for the first time the feasibility of applying ratiometric fluorophores to stimuli-responsive materials. With an increasing temperature, the

fluorescence colors of **PNIPAM** materials covalently labeled with 3-hydroxyflavones change from a bluish to greenish color, providing excellent sensitivity and reversibility. Moreover, the sensing temperature range lying in the range of 33 to 41 °C warrants applications in intracellular imaging. The ratiometric nature of the nanothermometer may successfully overcome certain difficulties encountered by conventional fluorescent molecular thermometers, ultimately providing a more robust signal. Further applications of this fluorescent nanothermometer in cell imaging are underway and will be reported in due course.

Notes and references

- (a) R. Liu, M. Fraylich and B. R. Saunders, *Colloid Polym. Sci.*, 2009, **287**, 627; (b) S. Aoshima and S. Kanaoka, *Adv. Polym. Sci.*, 2008, **210**, 169; (c) D. Schmaljohann, *Adv. Drug Delivery Rev.*, 2006, **58**, 1655; (d) A. M. Schmidt, *Colloid Polym. Sci.*, 2007, **285**, 953; (e) F. Fernández-Trillo, J. C. M. van Hest, J. C. Thies, T. Michon, R. Weberskirch and N. R. Cameron, *Chem. Commun.*, 2008, 2230; (f) Z. Hu, T. Cai and C. Chi, *Soft Matter*, 2010, **6**, 2115.
- (a) C. Gota, K. Okabe, T. Funatsu, Y. Harada and S. Uchiyama, *J. Am. Chem. Soc.*, 2009, **131**, 2766; (b) S. Uchiyama, Y. Matsumura, A. P. de Silva and K. Iwai, *Anal. Chem.*, 2003, **75**, 5926; (c) K. Iwai, Y. Matsumura, S. Uchiyama and A. P. de Silva, *J. Mater. Chem.*, 2005, **15**, 2796; (d) M. Onoda, S. Uchiyama and T. Ohwada, *Macromolecules*, 2007, **40**, 9651.
- (a) Y. Shiraishi, R. Miyamoto and T. Hirai, *Org. Lett.*, 2009, **11**, 1571; (b) Q. Yan, J. Yuan, Y. Kang, Z. Cai, L. Zhou and Y. Yin, *Chem. Commun.*, 2010, **46**, 2781.
- (a) L. Zhu, W. Wu, M.-Q. Zhu, J. J. Han, J. K. Hurst and A. D. Q. Li, *J. Am. Chem. Soc.*, 2007, **129**, 3524; (b) S. W. Hong, D. Y. Kim, J. U. Lee and W. H. Jo, *Macromolecules*, 2009, **42**, 2756; (c) T. Wu, G. Zou, J. Hu and S. Liu, *Chem. Mater.*, 2009, **21**, 3788; (d) L. Tang, J. K. Jin, A. Qin, W. Z. Yuan, Y. Mao, J. Mei, J. Z. Sun and B. Z. Tang, *Chem. Commun.*, 2009, 4974.
- (a) Y. Shiraishi, R. Miyamoto, X. Zhang and T. Hirai, *Org. Lett.*, 2007, **9**, 3921; (b) Y. Shiraishi, R. Miyamoto and T. Hirai, *Langmuir*, 2008, **24**, 4273; (c) D. Wang, R. Miyamoto, Y. Shiraishi and T. Hirai, *Langmuir*, 2009, **25**, 13176.
- (a) A. P. Demchenko, A. S. Klymchenko, V. G. Pivovarenko, S. Ercelen, G. Duportail and Y. Mély, *J. Fluoresc.*, 2003, **13**, 291; (b) A. S. Klymchenko, G. Duportail, A. P. Demchenko and Y. Mély, *Biophys. J.*, 2004, **86**, 2929.
- (a) L. Choulier, V. V. Shvadchak, A. Naidoo, A. S. Klymchenko, Y. Mély and D. Altschuh, *Anal. Biochem.*, 2010, **401**, 188; (b) K. Enander, L. Choulier, A. L. Olsson, D. A. Yushchenko, D. Kanmert, A. S. Klymchenko, A. P. Demchenko, Y. Mély and D. Altschuh, *Bioconjugate Chem.*, 2008, **19**, 1864.
- (a) P.-T. Chou, C.-H. Huang, S.-C. Pu, Y.-M. Cheng, Y.-H. Liu, Y. Wang and C.-T. Chen, *J. Phys. Chem. A*, 2004, **108**, 6452; (b) P.-T. Chou, W.-S. Yu, Y.-M. Cheng, S.-C. Pu, Y.-C. Yu, Y.-C. Lin, C.-H. Huang and C.-T. Chen, *J. Phys. Chem. A*, 2004, **108**, 6487.
- (a) A. S. Klymchenko, Y. Mély, A. P. Demchenko and G. Duportail, *Biochim. Biophys. Acta, Biomembr.*, 2004, **1665**, 6; (b) M. S. Celej, W. Caarls, A. P. Demchenko and T. M. Jovin, *Biochemistry*, 2009, **48**, 7465.